Numerical investigation of the behaviour of underground strata reinforced with polymer liner, steel mesh and bolts subjected to buckling failure

Saurav Karn
BHP, Adelaide, Australia

Ian Porter
University of Wollongong, Wollongong, Australia

Shivakumar Karekal
University of Wollongong, Wollongong, Australia

ABSTRACT: In this work, numerical models are developed to compare the support characteristics of a glass reinforced polymeric liner and steel mesh in supporting coal mine roof strata subject to buckling failure. The numerical models consisted of four plaster slabs bolted together and loaded under compression to mimic roof strata having rock bolts in a highly stressed mine roadway. The liner supported model showed greater stiffness and peak strength than the steel mesh model and were in good agreement with the experimental results. The bolts only and the steel mesh supported models were found to fail in tension with cracks originating near the centre of the outer slab and propagating inwards. However, as a result of strong bonding of the liner, no tensile cracks formed in the outer plaster slab and the liner supported model failed under shear alongside the interface of the liner.

Keywords: Thin spray-on liners, Fibre-reinforced polymers, Steel mesh, Numerical modelling, Buckling strata.

1 INTRODUCTION

The interaction of rock reinforcement and surface support plays an essential role in determining the effectiveness of an integrated ground support system in an underground working. Surface support such as steel mesh and shotcrete helps in containing the loose rock fragments, preventing them from falling on mining personnel working below and also resisting the surface deformation. Steel wire mesh, the most widely used form of surface support, is labour intensive and provides passive support. The passive support requires the rock mass to displace before it can provide any support reaction. A new generation of fast setting thin spray-on liner (TSL) is being developed at the University of Wollongong, which cures within seconds and when mixed with glass fibres provides active support.

In an underground coal mine the roadway failure mechanisms are mainly classified into six types: beam failure, joint-controlled rock falls, roof sag, guttering and shear failure, skin failure and rib spalling. Beam failure of weak bedding planes, buckling of bedded or delaminated rock roofs near the mid-span and guttering failure at the roadway corners are commonly encountered in a high-stress environment (Shen 2014). The support characteristics of a fibre reinforced polymer (FRP) and steel

mesh against buckling failure of coal mine roof strata were studied in a series of large-scale experiments at the University of Wollongong (Shan et al. 2019). This study attempts to simulate the support behaviour of the polymer liner and steel mesh in the buckling experiments using numerical models.

2 NUMERICAL MODEL

The numerical models consisted of an assembly of four hydrostone plaster slabs bolted together, with each slab having a 5° slope at the middle to initiate buckling. Three scenarios were considered to measure the resistance of the plaster assembly to buckling failure. In the first scenario, the plaster slabs were loaded under buckling load, supported only by the steel bolts. In the second and third scenarios, the plaster slabs were supported by the bolts and surface support was also applied using steel mesh and a fibre reinforced polymer (FRP) liner, respectively (see Figure 1).

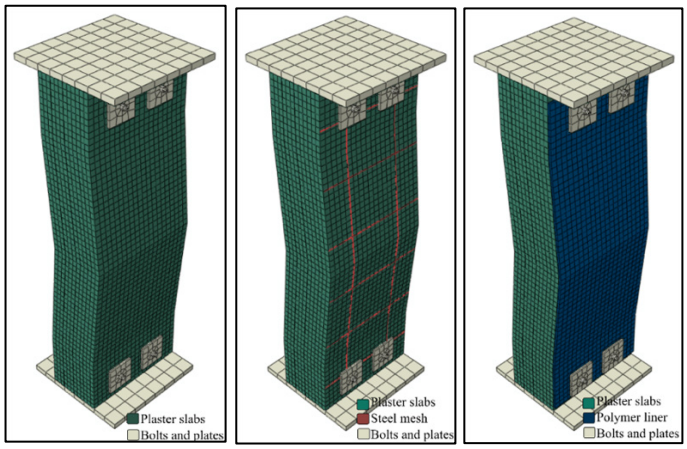

Figure 1. Numerical models simulating large scale buckling experiments.

The numerical models developed in this study consisted of four components: the substrate (hydrostone plaster slabs), the FRP liner, steel mesh and the interface between the liner and the substrate. Before modelling the large-scale experiments, material models for modelling the components were calibrated, and input parameters required were determined.

2.1 Material models

The concrete damaged plasticity (CDP) model (Lee & Fenves 1998 and Lubliner et al. 1989) available in ABAQUS was used to model the hydrostone plaster and polymer liner. The CDP model assumes two main failure mechanisms, tensile cracking and compressive crushing. The failure of the material is characterised by degrading the initial elastic stiffness, using two damage variables under compression and tension loads. Table 1 lists the mechanical properties used in the model.

Table 1. Mechanical properties of hydrostone plaster and polymer liner.

Properties		Hydrostone plaster	Polymer liner
Initial stiffness	[GPa]	18	3
Poisson's ratio		0.24	0.35
Tensile strength	[MPa]	8	40
Compressive strength	[MPa]	60	60
Inelastic strain at failure (compression)	[%]	0.34	-
Damage variable at failure (compression)		0.9	-
Inelastic strain at failure (tension)	[%]	0.15	-
Damage variable at failure (tension)		0.99	-

2.2 *Interface model*

The behaviour of the interface between the polymer and the plaster substrate is an important property which defines the support characteristic of the TSL. The polymer forms a strong bond with the substrate upon which it is applied. This ability of a TSL liner to adhere to the rock surface is classified into two types of bond strength, tensile bond strength and the shear bond strength. The interface between the polymer and plaster substrate was modelled using a cohesive zone model (Saurav et al. 2020). The damage evolution parameter, α, was back-calculated using numerical modelling. A series of numerical simulations were carried out with different values of α, modelling the double-sided shear test and the results obtained were compared against the experimental results (see Figure 2).

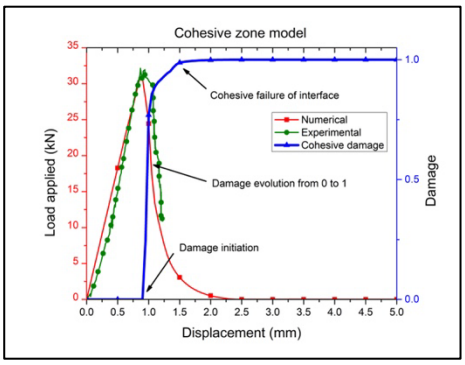

Figure 2. Calibration of interface parameters using cohesive zone model (Saurav et al. 2020).

2.3 *Steel mesh model*

Steel mesh section was used for supporting the plaster slabs in the buckling experiment. The numerical model developed for steel mesh was calibrated using a three-point bending test of steel wire. Steel mesh wires having diameter 5 mm and 7 mm were modelled using beam elements. An analytical solution for the three-point bend test was also used to verify the numerical results (Karampinos et al. 2018). The simulation results were in good agreement with both the analytical and the experimental results (see Figure 3).

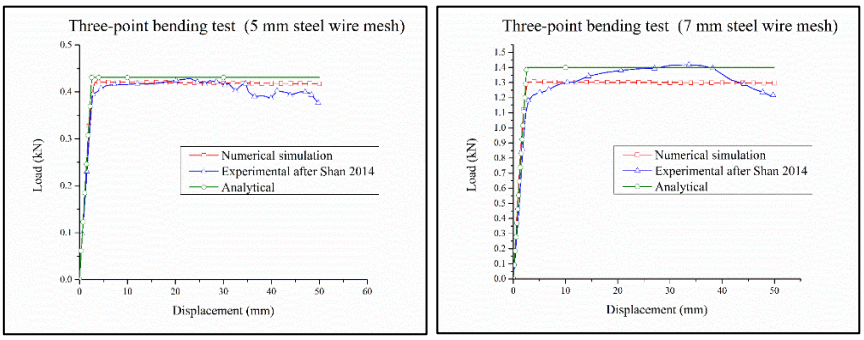

Figure 3. Three point bending tests: simulation, analytical and experimental.

A simulation of the full-scale pull test on the mesh section was carried out to validate the calibrated model for steel mesh wires. The steel mesh section consisted of 5 mm diameter longitudinal and transverse steel wires with 7 mm diameter longitudinal reinforcing steel wires at bearing plates. The mesh section was 1.35 m by 3.6 m, and the bolts were placed at 1 m span (see Figure 4). The mesh section was modelled using the beam structural elements with the calibrated input parameters, and bearing plates were simulated by fixing nodes near the bearing plates in three directions, to achieve no slippage of mesh at the bolts. Figure 4 compares the load vs displacement curve for numerical and experimental results after Shan et al. (2020). The failure load for the mesh section was found to be 44 kN in the experimental and 41 kN in the numerical simulation.

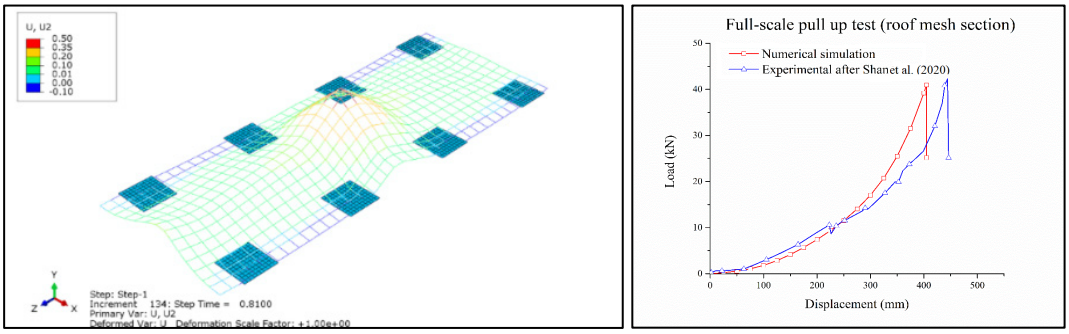

Figure 4. Full scale pull test on mesh sections: numerical and experimental.

2.4 Large scale numerical models

Four hydrostone plaster slabs were bolted together using bolts and plates and loaded. The load was applied in three steps in the numerical simulation. In the first step, a pre-tension of 1 kN was applied to the bolts and plates, so that the plaster slabs were clamped together during the application of load. In the second step, an initial displacement of 0.6 mm was applied on the top surface of the plaster slabs, and the behaviour of the plaster slabs was adjusted according to the estimated initial stiffness to account for the initial slack in the system observed during the experimental studies. After the initial slack stage, 2.4 mm displacement was applied in the third step, and the slabs were allowed to buckle. The damaged plasticity-based material model defined was used for the hydrostone in the third stage of loading. Overall displacement, u = 3 mm, was applied to the assembly. The steel mesh was modelled using the material parameters estimated from the calibrated steel mesh model. The polymer-supported assembly had a cohesive surface-based interface between the rightmost plaster slab and the polymer to simulate the behaviour of the interaction between them. The mechanical properties of the interface were taken from the calibrated interface model.

3 RESULTS AND DISCUSSIONS

The central area of the slabs was observed to be in tension, with the maximum tensile stress at the outermost surface of the right-most slab. No failure of plaster was observed during the pretension, and initial slack stages and the maximum tensile and compressive stresses were well below the respective yield values. As the load increased, a tensile crack initiated when the stresses reached the tensile strength of the hydrostone plaster. The tensile crack initiated at the outer surface of the rightmost slab and propagated through the whole assembly, as the load increased. The model failed immediately after the propagation of the cracks through the whole assembly. The model exhibited brittle failure as soon as the peak load was reached, similar to the experimental study (see Figure 5).

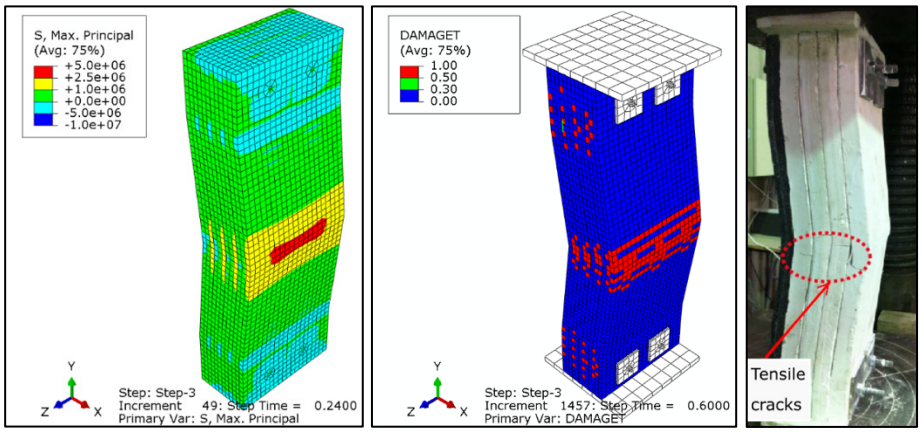

Figure 5. Failure behaviour of the bolts only supported model.

The steel mesh model failed in a similar manner to the bolts only model, with tensile cracks initiating in the rightmost plaster, at a cracking load of 90 kN and then developing in the other three slabs. Additional cracks developed around the bolting area with an increase in load (see Figure 6).

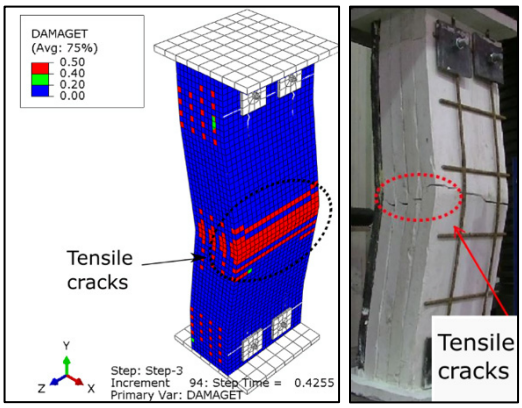

Figure 6. Failure behaviour of the bolts and steel mesh supported model.

As a result of bonding of the polymer liner with the outermost plaster slab, tensile cracks only began to form in the left-most slab at a relatively high load of 105 kN. In comparison, the mesh supported model had a cracking load of 90 kN and a peak load of 123 kN, which showed that the FRP liner delayed the formation of cracks in the plaster slabs. The FRP liner formed a composite system with the plaster, and the assembly kept on sustaining the increasing load. The tensile cracks propagated towards the right until the assembly reached a peak load of 201 kN. The crushing of plaster slabs due to compressive stress was also observed near the middle section. After the peak load, shear cracks propagated in the outer slab, along with the polymer interface. The inner plaster slabs failed in tension, and the rightmost slab bonded to the polymer liner failed in shear, similar to the experimental results (see Figure 7).

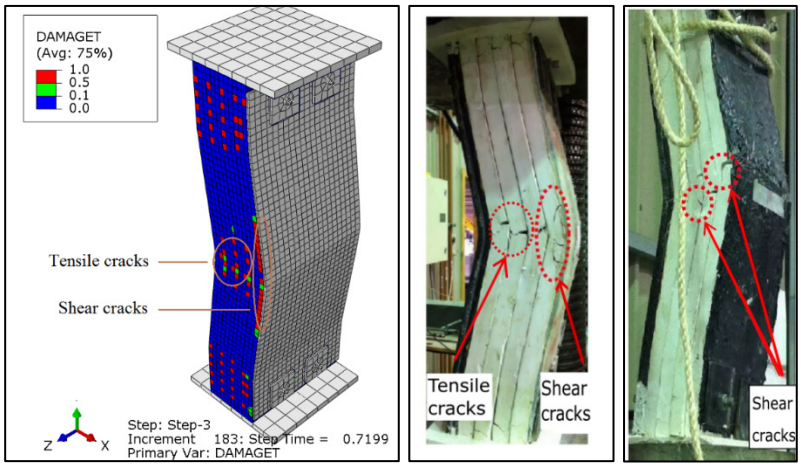

Figure 7. Failure behaviour of the bolts and TSL supported model.

The load vs vertical displacement curves obtained as a result of the simulation were compared against the experimental curves determined by Shan et al. (2019) (see Figure 8). The load at which initial cracks began to form in the bolts supported assembly was found to be 55 kN compared average load of 56 kN in the physical tests. The model sustained a peak load of 69 kN, compared to peak load of 63 kN observed in the experiment. The steel mesh supported model had a peak load of 123 kN, compared to the experimental value of 128 kN. The peak load observed in the mesh confined model was almost double that of the bolts only supported model. The model simulated in this case had almost no gap between the right-most slab and steel mesh, however, the gap between the mesh and the rock surface can affect the reinforcement capacity of the steel mesh. The peak load observed in

the physical tests was found to be 200 kN compared to the simulation peak load of 201 kN for the polymer liner supported assembly. The curves showed that the FRP supported model had higher stiffness and strength than the mesh and bolt only supported models. The bonding of the FRP with the outer plaster slab resisted the formation of tensile cracks in the slab, which increased the peak strength of the assembly.

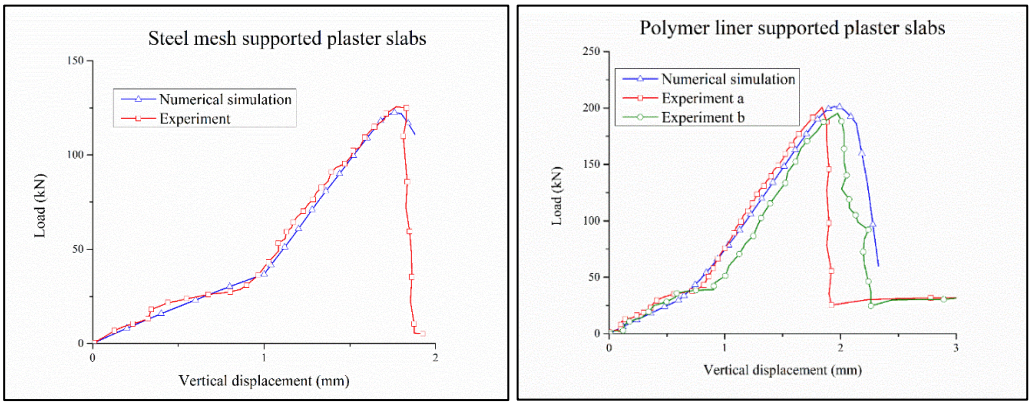

Figure 8. Comparison of buckling simulation results with experimental results.

4 CONCLUSIONS

The numerical simulations carried out in this study compares the reinforcement capacity of a polymer liner and steel mesh against buckling failure. The polymer liner had better performance over the steel mesh in restricting buckling failure. The polymer-supported model had higher crack initiating load, and thus, it can be concluded that the liner provided more effective reinforcement than the steel mesh in limiting failure due to buckling. The polymer model was observed to fail in shear which indicated that the liner was able to restrict the propagation of tensile cracks across the slabs, whereas the steel mesh model and bolts only model were observed to fail when tensile cracks initiated at the outer surface of the rightmost slab. The steel mesh was unable to confine the plaster slab, which indicated the inability of the steel mesh in providing support to the strata until a significant displacement has occurred. The polymer liner showed potential in replacing the steel mesh and provide active support to the strata immediately after application.

REFERENCES

Karampinos, E., Baek, B. & Hadjigeorgiou, J. 2018. Discrete element modelling of a laboratory static test on welded wire mesh. *In Proceedings of the Fourth International Symposium on Block and Sublevel Caving, Australian Centre for Geomechanics, Perth* 4, pp. 735-746.

Lee, J. & Fenves, G.L. 1998. Plastic-damage model for cyclic loading of concrete structures. *Journal of Engineering Mechanics* 124, pp. 892-900. DOI: 10.1061/(ASCE)0733-9399(1998)124:8(892)

Lubliner, J., Oliver, J., Oller, S. & Onate, E. 1989. A plastic-damage model for concrete. *International Journal of Solids and Structures* 25, pp. 299-326. DOI: 10.1016/0020-7683(89)90050-4

Shen, B. 2014. Coal mine roadway stability in soft rock: a case study. *Rock Mechanics and Rock Engineering* 47, pp. 2225-2238. DOI: 10.1007/s00603-013-0528-y

Shan, Z., Porter, I., Nemcik, J. & Baafi, E. 2019. Investigating the behaviour of fibre reinforced polymers and steel mesh when supporting coal mine roof strata subject to buckling. *Rock Mechanics and Rock Engineering* 52, pp. 1857-1869. DOI: 10.1007/s00603-018-1656-1

Shan, Z., Porter, I., Nemcik, J., Baafi, E. & Zhang, Z. 2020. Investigation on the Rock Surface Support Performance of Welded Steel Mesh and Thin Spray-On Liners Using Full-Scale Laboratory Testing. *Rock Mechanics and Rock Engineering* 53, pp.171-183. DOI: 10.1007/s00603-019-01895-5

Saurav, S., Porter, I. & Karekal, S. 2020. Cohesive zone modelling of a polymer-based liner interface using finite element analysis. In: *Proceedings of the ISRM International Symposium - EUROCK 2020*, June 2020.